1996

On the importance of chain reptation in models of dissolution of glassy polymers

Balaji Narasimhan, *Purdue University*
Nikolaos A. Peppas, *Purdue University*

On the Importance of Chain Reptation in Models of Dissolution of Glassy Polymers

Balaji Narasimhan and Nikolaos A. Peppas*

School of Chemical Engineering, Purdue University, West Lafayette, Indiana 47907

Received September 26, 1995; Revised Manuscript Received January 8, 1996[⊗]

ABSTRACT: Polymer dissolution was described by chain reptation incorporated into penetrant transport. The penetrant concentration field was divided into three regimes which delineate three different transport processes. Solvent penetration through the polymer was modeled to occur as a consequence of a diffusional flux and an osmotic pressure contribution. Species momentum balances were written that coupled the polymer viscoelastic behavior with the transport mechanism. Transport in the second penetrant concentration regime was modeled to occur in a diffusion boundary layer adjacent to the rubbery−solvent interface, where a Smoluchowski type diffusion equation was obtained. The disentanglement rate of the polymer is given by the ratio between the radius of gyration of the polymer and the reptation time. This rate was used to write the mass balance at the rubbery−solvent interface. Scaling law expressions for the disentanglement rate were derived. The model equations were numerically solved, and the effect of the polymer molecular weight and the diffusion boundary layer thickness on the dissolution mechanism was investigated for polystyrene dissolution in methyl ethyl ketone. The results showed that upon increasing the polymer molecular weight, the dissolution became disentanglement-controlled. Decrease in the diffusion boundary layer thickness led to a shift in the dissolution mechanism from disentanglement control to diffusion control.

Introduction

Polymer dissolution is an important phenomenon in polymer science and engineering. For example, in microlithographic applications, selectively irradiated regions of a photosensitive polymer are dissolved in appropriate solvents to obtain desired circuit patterns.[1] In the field of controlled drug release, zeroth-order drug release systems have been designed[2] by rendering the polymer dissolution phenomenon as the controlling step in the release process. Polymer dissolution also finds applications in membrane science,[3] treatment of unsorted plastics for recycling,[4] the semiconductor industry,[5] and packaging applications.[6]

The dissolution of a polymer in a solvent involves two transport processes, namely, solvent diffusion and chain disentanglement. When an uncross-linked, amorphous, glassy polymer is brought in contact with a thermodynamically compatible solvent, the latter diffuses into the polymer, and when the solvent concentration in the swollen polymer reaches a critical value, chain disentanglement begins to dominate and eventually the polymer is dissolved. Ueberrieter and co-workers[7−9] summarize the various types of dissolution and the surface structure of glassy polymers during dissolution. Important parameters like the polymer molecular weight, the solvent diffusion coefficient, the gel layer thickness, the rate of agitation, and the temperature were identified. Since then, various mathematical models have been proposed to understand polymer dissolution.

The approaches to model polymer dissolution can be broadly classified as (i) use of phenomenological models and Fickian equations, (ii) models with external mass transfer as the controlling resistance to dissolution, (iii) models based on stress relaxation, and (iv) analysis using anomalous transport models for solvent transport and scaling laws for actual polymer dissolution.

Tu and Ouano[10] proposed a phenomenological model with Fickian equations for polymer dissolution. They studied the motion of both the liquid−gel boundary and the gel−glass boundary. These boundaries were observed due to sharp changes in viscosity and refractive index at the surface. The important parameter in this model was the polymer disassociation rate, defined as the rate at which the polymer goes from a gel-like phase to a less viscous liquid solution. However, their simulations failed to quantitatively predict this disassociation rate from the molecular properties of the polymer. Devotta et al.[11] considered the Fickian dissolution of a spherical polymeric particle. They modeled chain "disengagement" by defining a flux that was proportional to the concentration of the polymer at the polymer−solvent interface. The transport of the chains in the solvent was assumed to be controlled by an external mass transfer resistance. Numerical simulations yielded the effect of the particle size on the dissolution process. The approach contained some parameters, the physical origin of which is unclear.

Lee and Peppas[12] proposed the idea of external mass transfer-controlled dissolution in their mathematical model. Fickian equations were used to describe the transport, and the diffusion of the polymer chains at the gel−liquid boundary was assumed to be controlled by the resistance offered by a liquid film. Approximate solutions of the model equations were obtained. Intuitive though the external mass transfer-controlled polymer dissolution approach may be, experiments have indicated that for dissolution of poly(methyl methacrylate) in methyl ethyl ketone,[13] vigorous agitation of the solvent increased the dissolution rate by only 15% relative to that for a stagnant solvent. Also, since the chain disentanglement mechanism was not considered, this approach failed to explain the swelling time needed before dissolution.

On the basis of the idea that polymer swelling due to solvent influx results in an elastic-like stress opposing the solvent penetration, Brochard and de Gennes[14] proposed relaxation-controlled polymer dissolution kinetics. The dissolution flux was expressed as the difference between the polymer stress gradient and the solvent osmotic pressure gradient. After the formation of a swollen gel layer, the sequential dissolution of the

* To whom all correspondence should be addressed.
[⊗] Abstract published in *Advance ACS Abstracts,* April 1, 1996.

0024-9297/96/2229-3283$12.00/0

polymer from the swollen state was assumed to be controlled by the local stress relaxation rate. This rate was shown to be of the order of the reptation time. Herman and Edwards[15] extended the above approach by considering in detail the stress accompanying the swelling of the polymer within the reptation model. They proposed that the solvent swelling induces a nonrandom distribution of polymer chain orientation. This contribution to the free energy and the chemical potential of the polymer and the solvent were evaluated in closed form using reptation theory. This approach could account for both solvent penetration and polymer dissolution but required several parameters that were difficult to measure experimentally.

Recognizing the presence of entanglements in polymers, dissolution has been understood as the transformation undergone by the polymer from an entangled gel-like phase to a disentangled liquid solution. The dynamics of these chains have been described by means of the reptation idea.[16] On the basis of the above arguments, Papanu et al.[17] proposed a reptation model for polymer dissolution. The dissolution rate was expressed as the ratio between the radius of gyration of the polymer and the reptation time. The dependence of the radius of gyration and the reptation time on the polymer molecular weight and the solvent concentration was derived using scaling laws.[18,19] The effective surface solvent concentration was identified as an important parameter and estimated by thermodynamics of the swollen network. Peppas et al.[20] recently proposed a polymer dissolution model, using an anomalous transport model for solvent penetration coupled with a reptation model for dissolution. The disentanglement time was proposed to be of the order of the reptation time. This model introduced the concept of the "dissolution clock" that controls the dissolution process and proposed that the magnitude of a "dissolution number" determined the gel layer thickness. This approach assumes that the solvent concentration at the polymer−solvent interface is independent of the solvent concentration history. Also, this approach fails to account for the decrease in the melt viscosity observed as a result of disentanglement.

A phenomenological model that accommodated molecular theories was recently proposed by Narasimhan and Peppas[21] to describe the dissolution of rubbery polymers. This approach delineated the concentration field into different regimes, and transport equations were written in each regime. Molecular arguments were used to predict the reptation diffusion coefficient and the disentanglement rate. The simulations indicated that the dissolution can be either disentanglement- or diffusion-controlled depending on the polymer molecular weight. This approach describes dissolution of rubbery polymers only, and the effects of a glass transition and the viscoelastic properties of the polymer on the dissolution process are not studied.

The objectives of the present research were (i) to develop a solvent transport model accounting for diffusional and relaxational mechanisms, in addition to effects of the viscoelastic properties of the polymer of the dissolution behavior, and (ii) to perform a molecular analysis of the polymer chain disentanglement mechanism, develop a mathematical model for polymer dissolution, and study the influence of various molecular parameters like the reptation diffusion coefficient, the disentanglement rate, and the gel layer thickness on the phenomenon.

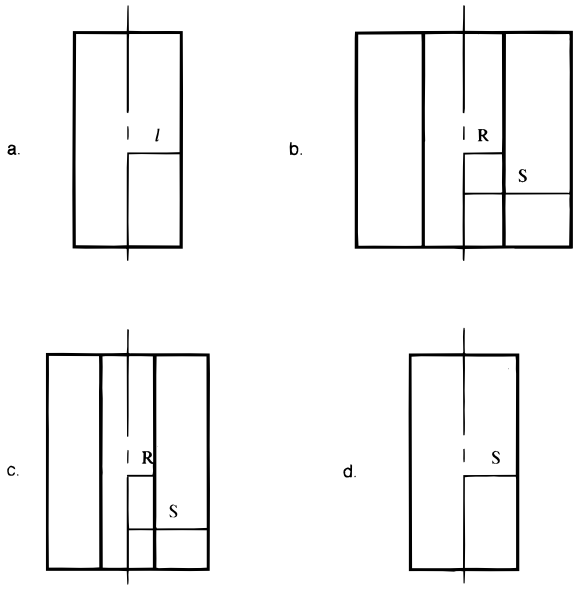

Figure 1. Schematic representation of a one-dimensional solvent diffusion and polymer dissolution process: (a) initial slab of thickness 2*l*, (b) initial swelling step showing the increasing position of the rubbery−solvent interface (*S*) and the decreasing position of the glassy−rubbery interface (*R*), (c) onset of the dissolution step showing the decreasing position of the interface *S* along with the decreasing position of the interface *R*, and (d) final dissolution step where the slab has been transformed into a rubbery material (disappearance of interface *R*) and the position of interface *S* still decreases.

Model Development

A model is developed for one-dimensional solvent diffusion in a thin polymer slab of thickness 2*l*. The solvent is component 1 and the polymer component 2. It is assumed that the molar volumes of the components remain constant during mixing.

The physical mechanism of the dissolution phenomenon is depicted in Figure 1. During the initial stage of the dissolution process, a glassy polymer of thickness 2*l* starts swelling due to the penetration of the solvent into it and the simultaneous transition from the glassy to the rubbery state. Thus two distinct fronts are observed—a swelling interface at position *R* and a polymer/solvent interface at position *S*. Front *R* moves inward while front *S* moves outward. When the concentration of the penetrant in the polymer exceeds a critical value, macromolecular disentanglement begins. After the concentration exceeds the critical value, true dissolution commences. After macromolecular disentanglement is complete, the polymer is dissolved. During this time, front *R* continues to move toward the center of the slab, while front *S* moves inward as well. After the disappearance of the glassy core, only front *S* exists, and it continues to move inward toward the center of the slab till all of the polymer is dissolved.

The entire concentration field is divided into three regimes. We define the swollen polymer (i.e., the region $R < x < S$ in Figure 1) as the "concentrated" regime. We postulate the existence of a diffusion boundary layer adjacent to the rubbery−solvent interface, *S*, through which the disentangled chains diffuse. The diffusion boundary layer is defined as the "semidilute" regime and has a constant thickness, δ. When the polymer is fully dissolved, the disentangled chains move freely in the solvent and exhibit Brownian motion. This region is referred to as the "dilute" regime. These regimes are depicted in Figure 2.

Model Equations in the Concentrated Regime. The continuity equation in one dimension for the solvent can be written as

$$\frac{\partial v_1}{\partial t} + \frac{\partial (v_1 v_1)}{\partial x} = 0 \qquad (1)$$

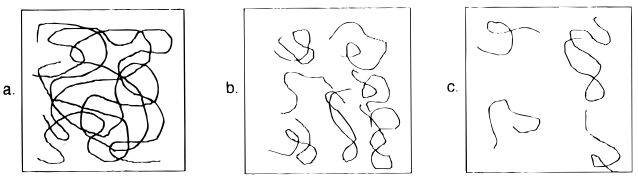

Figure 2. Disentanglement of polymer chains. (a) Before dissolution starts, there is no disentanglement; this is a swellable system. (b) Onset of disentanglement in the diffusion boundary layer occurs. (c) Dissolution is complete, and the disentangled chains exhibit Brownian motion in the solvent.

where v_1 is the volume fraction of the solvent and v_1 is the velocity of the solvent in the x-direction.

According to Fick's law,

$$j_{1,x} = -D_{12}\frac{\partial \rho_1}{\partial x} \tag{2}$$

where $j_{1,x}$ is the solvent mass diffusion flux relative to the volume-averaged velocity, D_{12} is the mutual diffusion coefficient, and ρ_1 is the mass of solvent per unit volume. The mutual diffusion coefficient, D_{12}, can be expressed as[22]

$$D_{12} = \frac{D_1 \rho_1 \rho_2 \hat{V}_2 \partial \mu_1}{RT \quad \partial \rho_1} \tag{3}$$

where D_1 is the self-diffusion coefficient of the solvent, μ_1 is the solvent chemical potential, V_2 is the specific volume of the polymer, R is the universal gas constant, and T is the temperature.

The equation for chemical potential of a penetrant in a swollen polymer is given as

$$\mu_1 = \mu_1^0 + RT\left[\ln v_1 + \left(1 - \frac{1}{x}\right)(1 - v_1) + \chi(1 - v_1)^2\right] + \overline{V}_1 \pi \tag{4}$$

Here, x is the number of monomer units per polymer chain, χ is the Flory solvent−polymer interaction parameter, and π is the osmotic pressure. Using eq 4 in eq 3, we obtain

$$D_{12} = D_1 v_2^2 (1 - 2\chi v_1) \tag{5}$$

The solvent flux relative to stationary coordinates is given by

$$v_1 v_1 = -\frac{D_1 v_1 v_2 \partial \mu_1}{RT \quad \partial x} \tag{6}$$

In the case where the solvent chemical potential is a function of both concentration and pressure, we have

$$v_1 v_1 = -\frac{D_1 v_1 v_2}{RT}\left[\frac{\partial \mu_1 \partial v_1}{\partial v_1 \, \partial x} + \frac{\partial \mu_1 \partial \pi}{\partial \pi \, \partial x}\right] \tag{7}$$

Rearranging the above equation and substituting eq 6 into it, we obtain

$$v_1 v_1 = -\left[D_{12}\frac{\partial v_1}{\partial x} + \frac{D_{12}\overline{V}_1 v_1 \qquad \partial \pi}{RT(1 - v_1)(1 - 2\chi v_1)\partial x}\right] \tag{8}$$

Thus, the solvent flux is expressed as a sum of contributions from diffusive and osmotic pressure terms. The osmotic pressure in the solvent flux expression depends upon the viscoelastic properties of the polymer. The relationship between the osmotic pressure and the stresses within the polymer can be derived by writing momentum balances.

The momentum balance for component i (i = 1, 2) is[23]

$$\rho_i \frac{D_i v_i}{Dt} = \nabla \mathbf{T}_i + \rho_i b_i + \rho_i p_i^+ \tag{9}$$

where $\mathbf{T}_i$ is the total stress tensor for component i, b_i is the body force, and p_i^+ is the exchange of linear momentum or diffusion drag between components. The total stress tensor of the solvent can be expressed as

$$\mathbf{T}_1 = -P_1 \mathbf{I} \tag{10}$$

where the shear stresses between the solvent molecules are assumed to be negligible because of slow flow. The total stress tensor of the polymer can be expressed as[24]

$$\mathbf{T}_2 = -P_2 \mathbf{I} + \sigma \tag{11}$$

where σ is the stress tensor of the polymer. For momentum conservation,

$$\rho_1 p_1^+ + \rho_2 p_2^+ = 0 \tag{12}$$

Adding the two-component balances yields

$$\nabla \pi = \nabla(P_1 + P_2) = \nabla \sigma - \left[\rho_1 \frac{D_1 v_1}{Dt} + \rho_2 \frac{D_2 v_2}{Dt}\right] + \rho_1 b_1 + \rho_2 b_2 \tag{13}$$

The inertial terms in the above equation are generally very small in penetrant diffusion in glassy polymers. For instance, if the acceleration rate is 0.01 m/s^2, the inertial term has a magnitude of 10 N/m^3. However, if the polymer is in the glassy state and the relaxation rate of the polymer is much slower than the penetrant diffusion rate, the stress difference at the glassy−rubbery interface can exceed 10^6 N/m^2, leading to a stress gradient of $>10^9$ N/m^3. In this case, the internal stresses are so high that some microcracks can be observed at the interface. Thus the inertial terms can safely be neglected, yielding

$$\nabla \pi = \nabla \sigma \tag{14}$$

In one dimension, the above equation reduces to

$$\frac{\partial \pi}{\partial x} = \frac{\partial \sigma_{xx}}{\partial x} \tag{15}$$

Substituting this equation into the solvent flux equation (eq 8), we observe that the flux is proportional to the gradient of the stress.

We have used the Maxwell model as the constitutive equation to describe viscoelastic behavior. In one dimension, this can be expressed as

$$\frac{\partial \sigma_{xx}}{\partial t} = -\frac{\sigma_{xx}}{\tau} + E\frac{\partial \epsilon_{xx}}{\partial t} \tag{16}$$

where τ is the Maxwell relaxation time and E is the spring modulus. τ and E are related as

$$\tau = \frac{\eta}{E} \tag{17}$$

The viscosity, η, is expressed as a function of the penetrant concentration, v_1, as

$$\eta = \eta_0 \exp(-a_\eta v_1) \tag{18}$$

where a_η is a plasticization parameter.

In continuum mechanics, the deformation gradient tensor, **F**, is used to relate the deformed state to the undeformed state.[25] Expressing this in one dimension, we can derive

$$\epsilon_{xx} = F_{11} - 1 = \frac{1}{v_2} - 1 \tag{19}$$

The above equation describes the coupling between the local deformation and the local penetrant concentration.

Substitution of the flux equation, eq 8, and the momentum balance equation, eq 15, into the mass balance equation, eq 1, yields

$$\frac{\partial v_1}{\partial t} = \frac{\partial}{\partial x}\left[D_{12}\frac{\partial v_1}{\partial x}\right] + \frac{\partial}{\partial x}\left[\frac{D_{12}\overline{V_1}v_1}{RT(1-v_1)(1-2\chi v_1)}\frac{\partial \pi}{\partial x}\right] \tag{20}$$

Then, by substituting eq 19 into the stress−strain constitutive equation, eq 16, we obtain

$$\frac{\partial \sigma_{xx}}{\partial t} = -\frac{\sigma_{xx}}{(\eta/E)} + \frac{E}{(1-v_1)^2}\frac{\partial v_1}{\partial t} \tag{21}$$

The above two equations represent the model equations for transport of solvent in the rubbery polymer, i.e., in the region $R < x < S$ as shown in Figure 1.

The kinetics of glass transition have been described by Astarita and Sarti[26] as

$$\frac{\mathrm{d}R}{\mathrm{d}t} = K(v_{1|x=R} - v_{1,t})^n \tag{22}$$

where $v_{1,t}$ is the solvent volume fraction corresponding to a threshold activity for swelling. K and n are the parameters of the kinetic model.

The appropriate initial and boundary conditions for the model eqs 20 and 21 are

$$t = 0,\ v_1 = v_{1,0},\ \sigma_{xx} = 0 \tag{23}$$

$$x = 0,\ \frac{\partial \sigma_{xx}}{\partial x} = 0 \tag{24}$$

$$x = R,\ (v_1 - v_{1,0})\frac{\mathrm{d}R}{\mathrm{d}t} = v_1 v_1,\ R(0) = 1 \tag{25}$$

$$x = S,\ v_1 = v_1^-,\ \sigma_{xx} = 0 \tag{26}$$

where v_1^- is the volume fraction of the solvent at the gel side of the gel−liquid interface.

Model Equations in the Diffusion Boundary Layer. As the polymer chains disentangle, they move out of the gel-like phase to a liquid solution through a diffusion boundary layer. The chain transport through this boundary layer is described as

$$\frac{\partial v_2}{\partial t} = \frac{\partial}{\partial x}\left[D_\mathrm{p}\frac{\partial v_2}{\partial x}\right] - \frac{\mathrm{d}S}{\mathrm{d}t}\frac{\partial v_2}{\partial x} \tag{27}$$

where D_p is the polymer diffusion coefficient in the solvent. The above equation is valid in a boundary layer of constant thickness δ, which can be estimated by the following relation:

$$\delta = \frac{k_1}{D_\mathrm{p}} \tag{28}$$

where k_l is a mass transfer coefficient.

The initial and boundary conditions for eq 27 are as follows:

$$t = 0,\ v_2 = 0 \tag{29}$$

At the end of the boundary layer, the conventional boundary condition is

$$x = S(t) + \delta,\ v_2 = 0 \tag{30}$$

The boundary condition on the solvent side of the gel−solvent interface can be written by considering that a polymer chain requires a minimum time to disentangle and move out of the gel. This minimum time is the reptation time.[19] Hence, the disentanglement rate is zero till a time equal to the reptation time elapses:

$$-D_\mathrm{p}\frac{\partial v_2}{\partial x} = 0,\ x = S^+(t),\ 0 < t < t_\mathrm{reptation} \tag{31}$$

After a time equal to the reptation time has elapsed, the transport of the chains at the gel−solvent interface may be disentanglement- or diffusion-limited. At times just greater than the reptation time, the rate of diffusion is sufficiently high, and hence the flux is disentanglement-limited. Hence, the boundary condition can be written as

$$-D_\mathrm{p}\frac{\partial v_2}{\partial x} = k_\mathrm{d},\ x = S^+(t),\ t > t_\mathrm{reptation} \tag{32}$$

where k_d is the disentanglement rate. An exact expression for k_d will be derived later.

As the disentanglement continues, the polymer concentration in the boundary layer increases till it reaches an equilibrium value, v_2^eq. At this instant, the diffusion rate becomes insufficient to transport the chains, and hence the polymer concentration is always maintained at v_2^eq. It is proposed that an equilibrium exists between the polymer rich gel and the polymer lean solvent in the diffusion boundary layer. Hence the boundary condition becomes

$$x = S^+(t),\ v_2^+ = v_2^\mathrm{eq},\ t > t_\mathrm{reptation} \tag{33}$$

The rubbery−solvent interface, S, moves due to the swelling of the polymer due to solvent ingress and by subsequent chain disentanglement. This can be expressed as

$$\frac{\mathrm{d}S}{\mathrm{d}t} = v_1 - \frac{D_\mathrm{p}}{v_1^-}\left(\frac{\partial v_2}{\partial x}\right)^+,\ S(0) = 1 \tag{34}$$

This completes the formulation of the moving boundary problem.

Interfacial Concentration. At the rubbery−solvent interface, there is thermodynamic equilibrium between the solvent and the polymer phases. Due to the presence of entanglements, the Flory−Huggins theory cannot be directly applied.

The change in the chemical potential of the solvent in the swollen polymer due to the presence of entanglements can be used to estimate the concentration at the rubbery−solvent interface.[27] As solvent penetration proceeds, there is a resistance due to the elastic deformation of the entangled chains, and the entangled network behaves like a permanent network for a short duration of time. This time scale is very small compared to the time scale of the dissolution process, and hence the Flory−Rehner theory can be applied in this situation.

The solvent chemical potential in a polymer−solvent mixture[17] is given by

$$\mu_1 = \mu_1^0 + RT\left[\ln v_1 + \left(1 - \frac{1}{x_n}\right)(1 - v_1) + \chi(1 - v_1)^2 + \frac{\overline{V_1}\,\nu_\mathrm{e}}{V_0 2N}\left(\frac{2}{1 - v_1} - (1 - v_1)\right)\right] \tag{35}$$

where the term $\nu_\mathrm{e}/2N$ is the moles of cross-links and N is the number of monomers per chain. Here, x_n is the ratio between the molar volume of the polymer and that of the solvent, and χ is the solvent−polymer interaction parameter.

The moles of cross-links are replaced with the moles of entanglements, and this can be expressed as

$$N_e = \frac{V_0\rho_2}{M}\left(\frac{M}{M_e} - 1\right) \tag{36}$$

where M_e is the molecular weight between entanglements. From rheological studies,[28]

$$M_e \sim \frac{M_c}{2} \tag{37}$$

where M_c is the critical molecular weight of the polymer, defined by a sharp increase in the slope of the viscosity vs the molecular weight curve, which is attributed to the onset of entanglements.[29] Hence, the chemical potential of the solvent is

$$\mu_1^- = \mu_1^0 + RT\left[\ln v_1 + \left(1 - \frac{1}{x_n}\right)(1 - v_1) + \chi(1 - v_1)^2 + \overline{V}_1\rho_2\left(\frac{2}{M_c} - \frac{1}{M}\right)\left(\frac{2}{1 - v_1}\right) - (1 - v_1)\right] \tag{38}$$

The chemical potential of the solvent in the diffusion boundary layer is calculated by a similar argument except that in this case, the entanglements are absent and, hence, there is no need to account for them. Therefore, the chemical potential of the solvent in the diffusion boundary layer can be written as

$$\mu_1^+ = \mu_1^0 + RT\left[\ln v_1 + \left(1 - \frac{1}{x_n}\right)(1 - v_1) + \chi(1 - v_1)^2\right] \tag{39}$$

By assuming that an equilibrium exists between the chemical potential of the solvent in the swollen polymer and that in the diffusion boundary layer, the solvent concentration on the gel side of the gel−liquid layer can be obtained.

Analysis of Diffusion Coefficient. It is necessary to appropriately define the diffusion coefficients that appear in all of the preceding transport equations. It can be demonstrated[21] that in dissolving systems there exists a critical solvent concentration, v_1^*, at which the mode of mobility of the polymer chains undergoes a change. This can be mathematically expressed as a change in the diffusivity.[21] This can be represented as

$$D_{12} = D_1,\ v_1 < v_1^* \tag{40}$$

$$D_{12} = D_2,\ v_1 > v_1^*$$

where

$$D_1 = D_0 \exp(a_d v_1) \tag{41}$$

where D_0 is the diffusivity of the solvent in a glassy polymer and D_2 is a "reptation" diffusion coefficient. An expression for the concentration and molecular weight dependence of D_2 can been derived[31] as

$$D_2 = \frac{A}{(1 - v_1)^{1.9}} \tag{42}$$

where A is a constant that depends on the polymer molecular weight, the solvent viscosity, and the temperature.

To determine the critical solvent concentration, v_1^*, at which the diffusivity changes to a reptative mode, the following argument is applied. The characteristic crossover concentration for a change from a concentrated to a semidilute solution for polymer melts[30] is used as an initial estimate for v_1^*:

$$v_1^* = \frac{3N}{4\pi r_g^3} \tag{43}$$

Here, N is the number of monomers, and r_g is the radius of gyration of the polymer.

The diffusion coefficient D_p that appears in the transport equations in the diffusion boundary layer is defined by treating the disentangling chains in the boundary layer as Brownian spheres. Thus, a Stokes−Einstein type diffusivity arises:

$$D_p = \frac{kT}{6\pi\eta_1 r_g} \tag{44}$$

Here, η_1 is the solvent viscosity, and r_g is the polymer radius of gyration. Using an exact expression for r_g,[21] D_p can be rewritten as

$$D_p = 1.1648 \times 10^{-14}\frac{T}{\eta_1 N^{0.5}} \tag{45}$$

where T is the temperature and N is the number of monomers in the chain.

We postulate that for a dissolving polymer, the disentanglement rate, k_d, can be given as the ratio of the radius of gyration, r_g, to the reptation time, $t_{reptation}$:

$$k_d = \frac{r_g}{t_{reptation}} \tag{46}$$

Exact expressions for r_g and $t_{reptation}$ have been derived elsewhere.[21] The final expression for the disentanglement rate is

$$k_d = \frac{B}{(1 - v_1)^{1.9}} \tag{47}$$

where B is a constant that depends on the polymer molecular weight, solvent viscosity, and temperature.

This completes the formulation of the problem with all parameters defined a priori except for the "equilibrium" concentration, v_2^{eq}, in the diffusion boundary layer. Owing to lack of any prior knowledge of this concentration, this is treated as a parameter. Hence we have formulated a one-parameter model through the foregoing arguments.

Numerical Simulations

Equations 20, 21, and 27 lead to a system of two coupled, nonlinear, partial differential equations, one of which is coupled with an ordinary differential equation. The solution of the above system of equations would also generate the temporal evolution of the two moving boundaries and hence the gel layer thickness. The concentration profiles can be integrated to obtain the mass of the polymer dissolved as a function of time. The moving boundary problem was transformed into a fixed boundary problem by using "front-fixing" techniques[31] that utilize a new set of space coordinates. A modified Landau transform[32] was applied to the concentrated regime, i.e., in the region $R < x < S$. This transform is given by

$$\xi_1 = \frac{x - R}{S - R} \tag{48}$$

This fixed the moving boundary as ξ_1 varies from 0 to 1. This transform is valid till the glassy core exists. Once the glassy core disappears, symmetry conditions for both the solvent concentration and the stress prevail at $x = 0$. The new Landau transform that fixes the rubbery solvent interface is

$$\xi_1 = \frac{x}{S} \tag{49}$$

A similar modified Landau transform was applied to the diffusion boundary layer, i.e., in the region $S < x <$

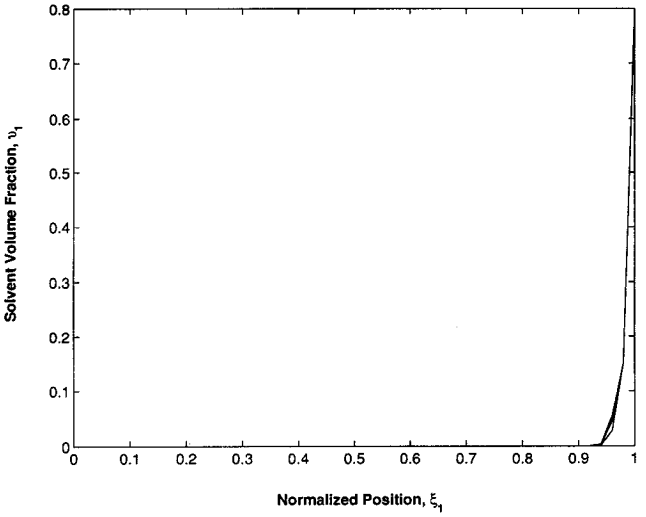

Figure 3. MEK volume fraction, v_1, as a function of normalized position, ξ_1. The polystyrene molecular weight was $\bar{M}_n$ = 52 000. The position $\xi_1 = 0$ is the center of the slab. The time increment starting from the first curve on the right is Δt = 1000 s.

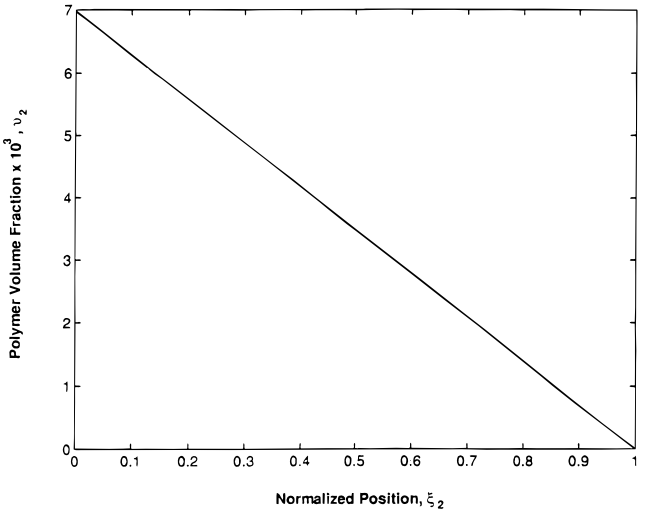

Figure 4. Polystyrene volume fraction, v_2, in the diffusion boundary layer as a function of normalized position, ξ_2. The polystyrene molecular weight was $\bar{M}_n$ = 52 000. The position $\xi_2 = 0$ represents the initial half-thickness of the slab.

$S + \delta$. The transform is given by

$$\xi_2 = \frac{x - S}{\delta} \tag{50}$$

This fixed the moving boundary as ξ_2 varies from 0 to 1 and is valid even after the polymer becomes completely rubbery. These transforms suitably modified the model equations. A fully implicit backward time-centered space finite difference technique was then utilized to transform the set of differential equations to a set of nonlinear algebraic equations at each time step. The details of the numerical algorithm are presented elsewhere.[33] The resulting system was solved by using the Thomas algorithm.[34]

To perform simulations with the model, the system methyl ethyl ketone (MEK)/polystyrene was used as a model system. Therefore, relevant thermodynamic and structural parameters were determined independently for this system at 25 °C. The MEK−polystyrene interaction parameter,[35] χ, was 0.49, and the M_c for polystyrene[36] was 38 000. The preexponential factor for the diffusion coefficient (see eq 41) was taken as 4×10^{-10} cm^2/s, and the exponential factor was chosen as 7. The interfacial concentration, v_1^-, was calculated to be 0.796 for polystyrene of molecular weight 52 000. The thickness of the diffusion boundary layer was chosen to be 5% of the initial half thickness of the slab. The modulus, E, was taken as 3×10^8 Pa, and the preexponential factor for the viscosity (see eq 18) was chosen as 25. Exact expressions[31] were used to calculate the reptation time, the disentanglement rate, and the Stokes−Einstein diffusion coefficient.

The effect of the polymer molecular weight on the dissolution mechanism was investigated. Figure 3 shows the solvent concentration profile in the polymer ($\bar{M}_n$ = 52 000) as a function of normalized position based on the undeformed coordinate system. The center of the slab is at $\xi_1 = 0$, and the rubbery−solvent interface is at $\xi_1 = 1$. Dramatic changes in the concentration profile are observed at the glassy−rubbery interface. The steep profiles are indicative of a relaxation-controlled dissolution mechanism, thus leading to case II type behavior. The flat profiles in the rubbery region have been attributed to very small diffusional resistance. The glassy core essentially behaves like an impervious wall, and as diffusional resistance increases, smoother concentration profiles are observed. Figure 4 shows a plot of the polymer volume fraction in the diffusion boundary layer as a function of the undeformed coordinate, ξ_2. The gradient of the polymer concentration becomes constant once the profiles fully develop, as is expected of boundary layer profiles. The stress profiles are shown in Figure 5. It is observed that the maximum stress level is at the interface. Figure 6 shows the temporal evolution of the glassy−rubbery interface, R, the rubbery−solvent interface, S, and the gel layer thickness, defined as ($S - R$). The concentration profiles were integrated to obtain the fraction of polymer dissolved, and this is shown in Figure 7. The profile is linear, once again providing evidence of case II transport. A more extended discussion of typical case II behavior during solvent transport through glassy polymers was recently provided by Rossi et al.[37]

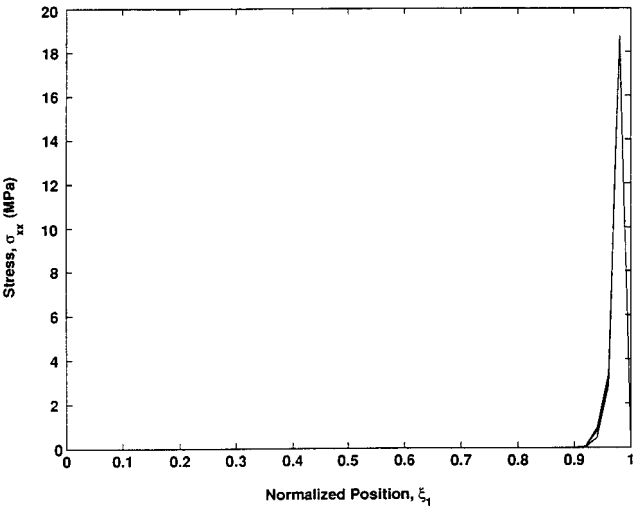

Figure 5. Internal stress, σ_{xx}, as a function of normalized position, ξ_1. The polystyrene molecular weight was $\bar{M}_n$ = 52 000. The position $\xi_1 = 0$ represents the center of the slab. The time increment starting from the first curve on the right is Δt = 1000 s.

As the polymer molecular weight is increased to 520 000, the reptation time increases and hence the diffusion coefficient decreases. The solvent concentra-

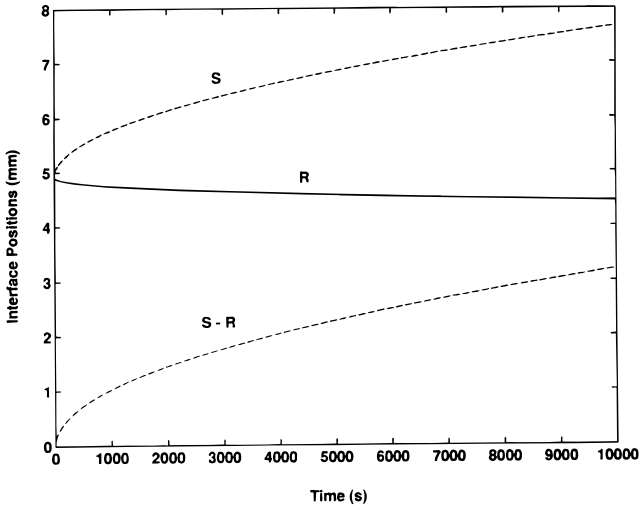

Figure 6. Rubbery−solvent interface (S), glassy−rubbery interface (R), and gel layer thickness ($S - R$) as a function of dissolution time. The polystyrene molecular weight was $\bar{M}_n$ = 52 000.

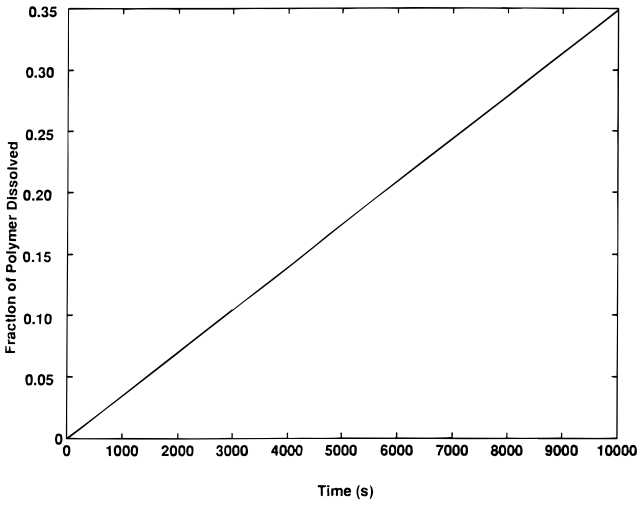

Figure 7. Fraction of polystyrene dissolved as a function of time. The polymer molecular weight was $\bar{M}_n$ = 52 000.

tion profiles in this case (Figure 8) are not as well developed, as the chains take much longer to disentangle and reptate out. The velocity of the moving interfaces also decreases as shown in Figure 9. The mass fraction of the polymer dissolved decreases with increase in the molecular weight as expected (Figure 10). Also, with increase in the molecular weight, the dissolution starts shifting toward a disentanglement-controlled mechanism as is seen from the thicker gel layer thicknesses. For polymer of molecular weight 1 040 000, the concentration profile is steep (Figure 11) and the gradient of the interface with time drastically decreases. This is as expected as the gradient (and hence the thickness of the gel layer) is controlled by the ratio of the diffusivity in the gel to that in the diffusion boundary layer. The fractional release profiles in Figure 12 show that until the reptation time elapses, no polymer dissolves. The dissolution mechanism in this case is completely disentanglement-controlled. It is interesting to observe that as the mechanism shifts to a disentanglement-controlled one, evidences of case II transport still persist.

The effect of the diffusion boundary layer thickness on the dissolution mechanism was studied. Figure 13 shows the solvent concentration profile in the swollen

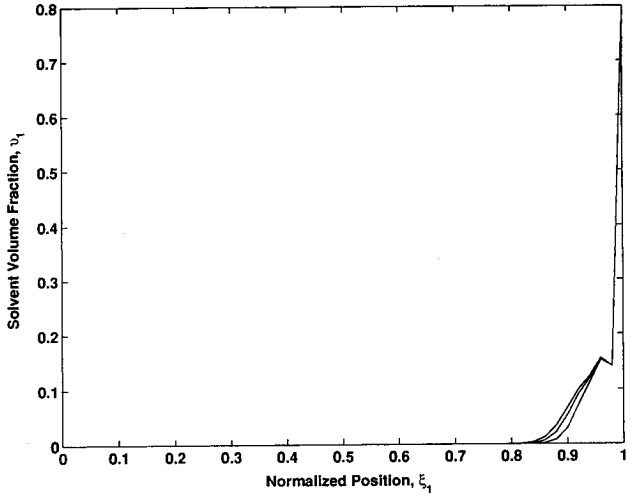

Figure 8. MEK volume fraction, v_1, as a function of normalized position, ξ_1. The polystyrene molecular weight was $\bar{M}_n$ = 520 000. The position $\xi_1 = 0$ is the center of the slab. The time increment starting from the first curve on the right is Δt = 5000 s.

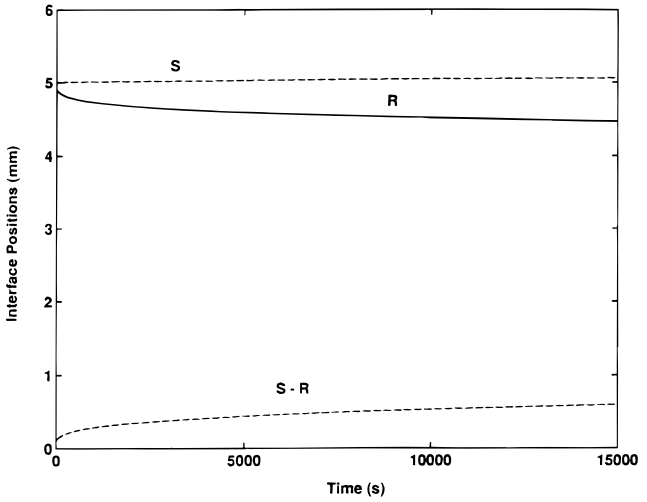

Figure 9. Rubbery−solvent interface (S), glassy−rubbery interface (R), and gel layer thickness ($S - R$) as a function of dissolution time. The polystyrene molecular weight was $\bar{M}_n$ = 520 000.

polymer ($\bar{M}_n$ = 520 000) for a diffusion boundary layer thickness that is 25% of the initial half-thickness of the polymer slab. Integrating this profile, we obtain the fraction of the polymer dissolved with time (Figure 14). Comparing this profile to that in Figure 10, it is observed that the mass of polymer dissolved has decreased. So even though the polymer molecular weight was unchanged, the dissolution rate dropped due to increased diffusional resistance through the boundary layer. This is typical of disentanglement control. Hence, diffusion-controlled dissolution can be achieved for high molecular weight polymers if the boundary layer thicknesses are high enough. This also shows a transition from case II transport to Fickian behavior. This is as expected as the mechanism is diffusion-controlled.

Conclusions

A new mathematical model to describe the dissolution of glassy polymers was developed by incorporating the mechanisms of chain disentanglement and reptation. The dissolution was envisaged to occur due to solvent penetration and subsequent chain disentanglement. The

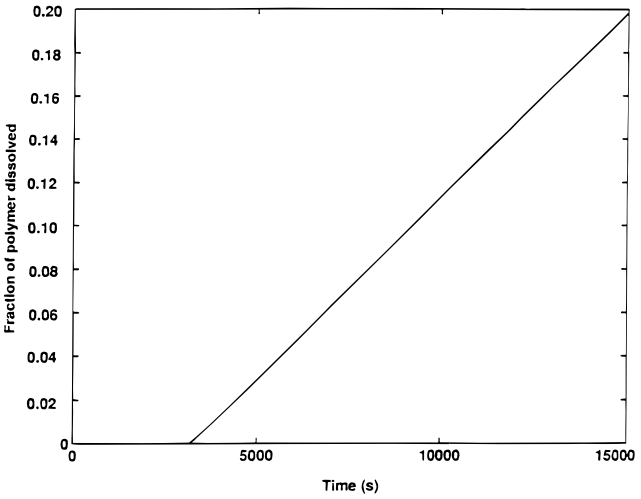

Figure 10. Fraction of polystyrene dissolved as a function of time. The polymer molecular weight was $\bar{M}_n = 520\,000$.

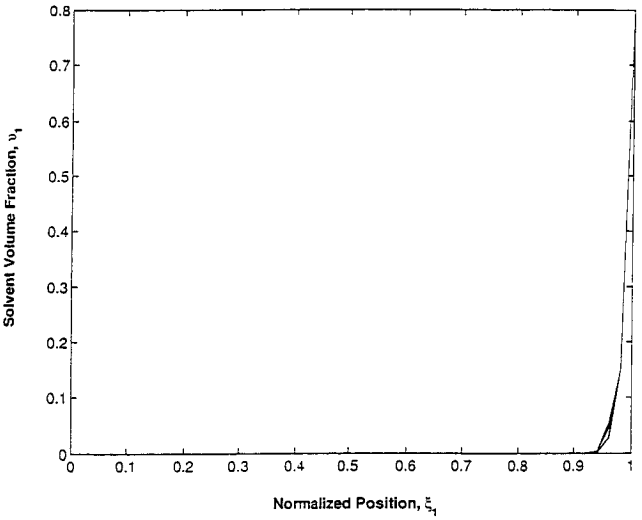

Figure 11. MEK volume fraction, v_1, as a function of normalized position, ξ_1. The polystyrene molecular weight was $\bar{M}_n = 1\,040\,000$. The position $\xi_1 = 0$ is the center of the slab. The time increment starting from the first curve on the right is $\Delta t = 10000$ s.

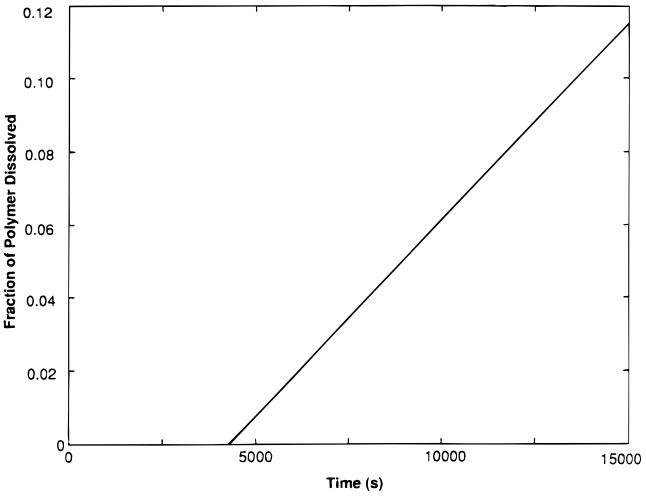

Figure 12. Fraction of polystyrene dissolved as a function of time. The polymer molecular weight was $\bar{M}_n = 1\,040\,000$.

penetrant concentration field was divided into three regimes which delineate three distinctly different transport processes. A continuum mechanics- based approach was used to treat solvent penetration in the swollen polymer. The solvent flux was expressed as the sum of contributions due to diffusion and osmotic pressure. The effect of the viscoelastic properties of the polymer on the transport was studied by coupling the solvent mass balance with an appropriate constitutive equation for the polymer. Molecular arguments were invoked to derive expressions for the diffusivity, the reptation time, and the disentanglement rate. Transport in the second penetrant regime was modeled to occur in a diffusion boundary layer adjacent to the rubbery−solvent interface. A fully implicit numerical technique was developed to solve the model equations, and the simulations were used to study the effect of the polymer molecular weight and the thickness of the diffusion boundary layer on the dissolution mechanism for polystyrene dissolution in MEK. The simulations demonstrated that the dissolution mechanism was disentanglement-controlled for higher molecular weight polymers and shifted to diffusion-controlled behavior on increasing the diffusion boundary layer thickness. This was observed by the difference in the profiles of the

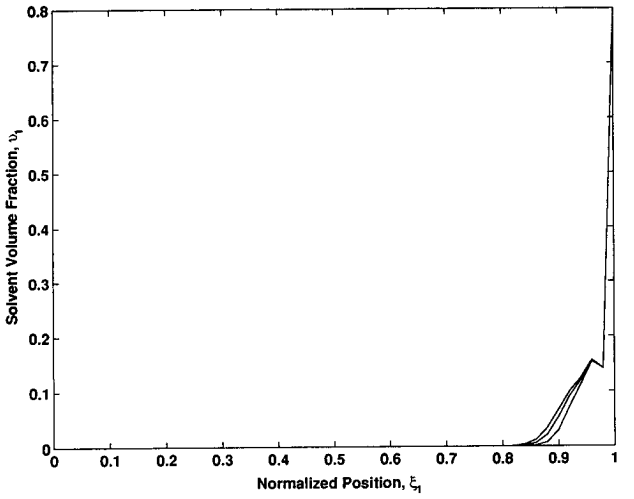

Figure 13. MEK volume fraction, v_1, as a function of normalized position, ξ_1. The polystyrene molecular weight was $\bar{M}_n = 520\,000$. The position $\xi_1 = 0$ is the center of the slab. The thickness of the diffusion boundary layer was 25% of the initial half-thickness of the polystyrene slab. The time increment starting from the first curve on the right is $\Delta t = 5000$ s.

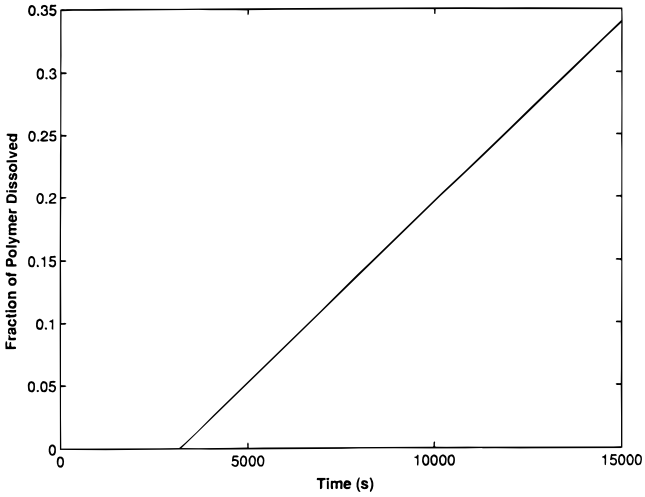

Figure 14. Fraction of polystyrene dissolved as a function of time. The polymer molecular weight was $\bar{M}_n = 520\,000$. The thickness of the diffusion boundary layer was 25% of the initial half-thickness of the polystyrene slab.

fraction of polymer dissolved with time. The mechanism of MEK penetration into polystyrene was established to be of the case II type though the dissolution process shifted to a Fickian mode on increasing the diffusion boundary layer thickness.

Acknowledgment. This work was supported in part by Grant No. CTS-92-12842 from the National Science Foundation. We wish to thank Professor Gianni Astarita of the University of Naples for valuable discussions and suggestions.

References and Notes

(1) O'Brien, M. J.; Soane, D. S. Resists in Microlithography. In *Microelectronics Processing: Chemical Engineering Aspects*; Hess, D. W., Jensen, K. F., Eds.; Am. Chem. Soc. Adv. Chem. Series 221; American Chemical Society: Washington, DC, 1989; pp 325−376.
(2) Colombo, P.; Catellani, P. L.; Peppas, N. A.; Maggi, L.; Conte, U. *Int. J. Pharm.* **1992**, *88*, 99.
(3) Tsay, C. S.; McHugh, A. J. *J. Polym. Sci., Polym. Phys. Ed.* **1990**, *28*, 1327.
(4) Nauman, E. B.; Lynch, J. C. PCT Int. Appl. WO 91 03 515 (U.S.Appl. 406.087, Sept. 11, 1989).
(5) Yeh, T. F.; Reiser, A.; Dammel, R. R.; Pawlowski, G.; Roeschert, H. *Macromolecules* **1993**, *26*, 3862.
(6) Wielgolinski, L. *Polym. Prepr. (Am. Chem. Soc., Div. Polym. Chem.)* **1991**, *32* (2), 15.
(7) Ueberreiter, K. The Solution Process. In *Diffusion in Polymers*; Crank, J., Park, G. S., Eds.; Academic Press: New York, 1968.
(8) Ueberreiter, K.; Asmussen, F. *J. Polym. Sci.* **1962**, *57*, 187.
(9) Asmussen, F.; Ueberreiter, K. *J. Polym. Sci.* **1962**, *57*, 199.
(10) Tu, Y. O.; Ouano, A. C. *IBM J. Res. Dev.* **1977**, *21*, 131.
(11) Devotta, I.; Ambeskar, V. D.; Mandhare, A. B.; Mashelkar, R. A. *Chem. Eng. Sci.* **1994**, *49*, 645.
(12) Lee, P. I.; Peppas, N. A. *J. Contr. Rel.* **1987**, *6*, 201.
(13) Papanu, J. S.; Hess, D. W.; Soane, D. S.; Bell, A. T. *J. Electrochem. Soc.* **1989**, *136*, 3077.
(14) Brochard, F.; de Gennes, P. G. *Physicochem. Hydrodyn.* **1983**, *4*, 313.
(15) Herman, M. F.; Edwards, S. F. *Macromolecules* **1990**, *23*, 3662.
(16) De Gennes, P. G. *J. Chem. Phys.* **1971**, *55*, 571.
(17) Papanu, J. S.; Soane, D. S.; Bell, A. T.; Hess, D. W. *J. Appl. Polym. Sci.* **1989**, *38*, 859.
(18) De Gennes, P. G. *Scaling Concepts in Polymer Physics*; Cornell University Press: Ithaca, NY, 1979.
(19) De Gennes, P. G.; Leger, L. *Annu. Rev. Phys. Chem.* **1982**, *33*, 49.
(20) Peppas, N. A.; Wu, J. C.; von Meerwall, E. D. *Macromolecules* **1994**, *27*, 5626.
(21) Narasimhan, B.; Peppas, N. A. *J. Polym. Sci., Polym. Phys. Ed.*, in press.
(22) Duda, J. L.; Vrentas, J. S.; Ju, S. T.; Liu, T. *AIChE J.* **1982**, *28*, 279.
(23) Mueller, I. *Arch. Rat. Mech. Anal.* **1968**, *28*, 1.
(24) Bird, R. B.; Armstrong, R. C.; Hassager, O. *Dynamics of Polymeric Liquids, Volume 1: Fluid Mechanics*; John Wiley: New York, 1987.
(25) Malvern, L. E. *Introduction to the Mechanics of a Continuous Medium*; Prentice-Hall: Englewood Cliffs, NJ, 1969.
(26) Astarita, G.; Sarti, G. C. *Polym. Eng. Sci.* **1978**, *18*, 388.
(27) Flory, P. J. *Principles of Polymer Chemistry*; Cornell University Press: Ithaca, NY, 1953.
(28) Graessley, W. W. *Adv. Polym. Sci.* **1974**, *16*, 1.
(29) Caramella, C.; Ferrari, F.; Bonferoni, M. C.; Ronchi, M.; Colombo, P. *Boll. Chim. Farm.* **1989**, *128*, 298.
(30) Des Cloizeaux, J.; Jannink, G. *Polymers in Solution: Their Modeling and Structure*; Oxford University Press: New York, 1990.
(31) Crank, J. *Free and Moving Boundary Problems*; Oxford University Press: New York, 1984.
(32) Landau, H. G. *Q. Appl. Math.* **1950**, *8*, 81.
(33) Narasimhan, B.; Peppas, N. A. Submitted to *Chem. Eng. Sci.*
(34) Hoffman, J. D. *Numerical Methods for Engineers and Scientists*; McGraw Hill: New York, 1992.
(35) Parsonage, E. E.; Peppas, N. A. *Br. Polym. J.* **1987**, *19*, 469.
(36) Lustig, S. R.; Caruthers, J. M.; Peppas, N. A. *Chem. Eng. Sci.* **1992**, *47*, 3037.
(37) Rossi, G.; Pincus, P. A.; de Gennes, P.-G. *Europhys. Lett.* **1995**, *32*, 391.

MA951450S